International Journal of Microwave and Wireless Technologies

cambridge.org/mrf

Switchable design of a frequency reconfigurable broadband whip antenna in high frequency

Hengfeng Wang and Chao Liu

Naval University of Engineering, College of Electronic Engineering, Wuhan 430033, China

Research Paper

Cite this article: Wang H, Liu C (2021). Switchable design of a frequency reconfigurable broadband whip antenna in high frequency. *International Journal of Microwave and Wireless Technologies* **13**, 454–462. https://doi.org/10.1017/S1759078720001117

Received: 12 February 2020
Revised: 24 July 2020
Accepted: 28 July 2020
First published online: 24 August 2020

Key words:
Broadband antenna; frequency reconfigurable technology; grasshopper optimization algorithm; lumped load; matching network; switchable technology

Author for correspondence:
Hengfeng Wang,
E-mail: henvin999@163.com

Abstract

In this paper, the antenna reconfigurable technology is used to redesign a whip antenna in different sub-bands of high frequency (HF). According to the electrical characteristics of the antenna, on the one hand, two different radiation whip heights are designed to solve the problem of pattern up-warping in the high-frequency band; on the other hand, a common upper loading network and several different adjusting inductors and matching networks are designed for each sub-band to achieve high gain and efficiency when keeping good voltage standing wave ratio (*VSWR*) characteristics. Five sub-bands of the 10-m HF whip antenna are reconfigured through the actual selection of radiation height, adjusting inductance, and matching network by radio frequency (RF) switch. The antenna load and matching network are optimized by grasshopper optimization algorithm (GOA), and integrated into the antenna body by using the printed circuit technology. The scaled prototype of 1 m frequency reconfigurable antenna is manufactured and tested, which shows that the *VSWR* is all <3 with an average value of 2.14; the gain is all >−2.5 dB with an average value of 3.90 dB; the efficiency is all >18.2% with an average value of 71.59%, and the patterns all keep horizontal omnidirectional without the phenomenon of up-warping.

Introduction

Whip antenna is a kind of special antenna with omnidirectional pattern in the horizontal direction, which has been widely used because of its simple structure, solid texture, suitable for installation, and use on mobile carriers [1]. With the wide application of frequency hopping, spread spectrum and other technologies in the short-wave communication system, the tuned antenna cannot meet the current communication needs. Therefore, the demand for high efficiency and broadband antenna becomes more and more urgent [1–4]. With standing wave current distribution, the working band limitation of whip antenna is mainly caused by impedance characteristics [1, 2], because it is very sensitive to the change of frequency. In the lower frequency band, the electric length is small, far less than 1/4 wavelength, the input resistance is small, and the input capacitive reactance is large, which makes it difficult to match with the feeder line. In the higher frequency band, the electric length is far greater than 1/4 wavelength, the reverse current on the vibrator is constantly increasing, and the maximum direction of the antenna pattern gradually deviates from the horizontal direction, which makes the antenna not satisfy middle/ short-range communication.

In order to improve the bandwidth and radiation performance of the antenna, top-loading [3–5], loading network [6–8], broadband matching network [9–11], fractal technology [12–14], and other methods have been proposed. At present, loading and matching network technology is widely used, because the introduction of impedance elements greatly improves the standing wave, but it brings new loss to the antenna and greatly reduces its gain and efficiency. In [15], the loading and matching network optimization design of whip antenna in the whole short wave has realized good bandwidth, but obviously, the gain and efficiency of low-frequency band and radiation pattern of the high-frequency band have been abandoned, so the whole short band has not been well taken into account. In [16], broadband loaded monopole antenna is introduced with three different lumped loads and a simple input matching network, whose *VSWR* is <2.5, but the lowest gain is only −10 dB. For this kind of antenna with a wide frequency band, it is often achieved by sacrificing gain and efficiency to achieve impedance broadband.

However, the emergence of frequency reconfigurable technology [17–22] undoubtedly provides a way to solve the above problem. In principle, the more sub-bands, the better the performance of the antenna, but the more complex the structure of the antenna, considering the radiation performance and implementation complexity of the reconfigurable antenna, a new reconfigurable broadband whip antenna is designed, which has a 10-m height, the band of

CAMBRIDGE UNIVERSITY PRESS

the antenna is divided into multiple sub-bands to improve their electrical characteristics respectively.

In this paper, the structure of the 10-m whip antenna is redesigned by using the antenna frequency reconfigurable technology. According to the electrical characteristics of the whip antenna, the working frequency band (high frequency) is divided into five sub-bands, on the one hand, two different radiation whip heights are designed to solve the problem of pattern up-warping in the higher frequency band; on the other hand, a common upper loading network and several different adjusting inductors and matching networks are designed for each sub-band to achieve higher gain and efficiency when keeping good impedance characteristics. All the parameters are optimized respectively by GOA to further improve the electrical characteristics in each sub-band, and the selection of radiator height and each network will be determined by the RF switches according to the actual needs. Finally, a scaled prototype of 1-m whip antenna is fabricated, the measured results show *VSWR* ?3, gain ≥2.5 dB, and the patterns all keep horizontal omnidirectional without the phenomenon of up-warping.

Antenna design

The working frequency of the 10-m HF whip antenna is 3–30 MHz, which is up to 10 octaves. The input impedance calculated in the electromagnetic simulation software FEKO has shown in Fig. 1, which varies greatly with frequency. In the lower frequency band, the input resistance is very small, the minimum is only 3.98 Ω (at 3 MHz), the input capacitive reactance is very large, the maximum is −390 Ω (at 3 MHz), which is difficult to match with the 50 Ω feeder. Therefore, the frequency reconfigurable technology can be introduced to divide the HF band, each sub-band is configured with a set of corresponding adjustable inductance L_0 (compensating excessive capacitive reactance) and matching network, so the difficulty of impedance matching with a smaller frequency range will be greatly reduced. When the frequency is 15 MHz, the input capacitive reactance is also very large, as high as −484 Ω and the antenna has a relatively large input resistance of 423 Ω, but the impedance matching difficulty of the high-frequency band is not as large as that of the lower-frequency band relatively, because transmission line transformer and matching network will make the antenna have a better impedance bandwidth.

Reactance loading can improve broadband characteristics and reduce the sensitivity of the loading point to the frequency change, while the resistance loading is a frequency-independent component, which can widen the working frequency band. The efficiency of reactance loading antenna is high, but its bandwidth is narrow, and the bandwidth of resistance loading antenna is wide, but its efficiency is very small, so we can adopt a mixed load with inductance and resistance to achieve high efficiency and wideband antenna. In addition, loading a larger resistance can improve the input resistance and achieve better matching with 50 Ω feeder, but the introduction of the resistance increases the power loss and then greatly reduces the gain and efficiency. As the current on the antenna body decreases with the increase of the height of the antenna, the higher the height of the load resistor, the smaller the loss will be. Therefore, the load network must be set on the upper part of the antenna, and the load resistor should be as small as possible on the premise of satisfying the impedance matching, and the load quantity should be as small as possible to reduce the complexity and instability of the antenna structure.

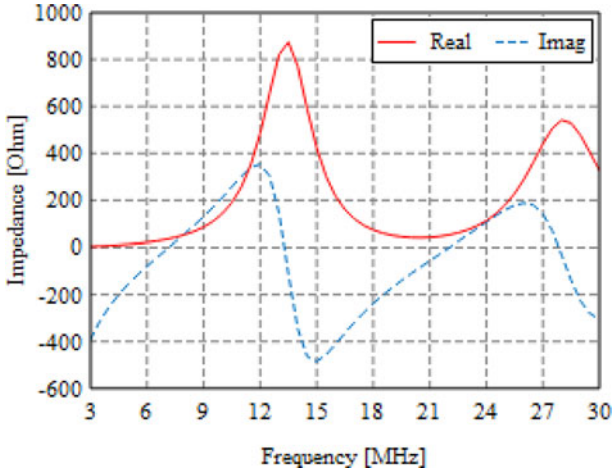

Fig. 1. Input impedance of 10 m whip antenna.

The structure of the proposed frequency reconfigurable whip antenna is shown in Fig. 2, which is composed of a RL loading network located at 1/4 from the top of the antenna. Moreover, a network composed of transformer and reactance elements can be used to further improve the impedance matching, an adjusting inductance L_0 can be added at the bottom of the antenna to compensate its high capacitance.

According to the input impedance distribution in Fig. 1, the lower frequency band of the proposed antenna is divided into three bands (I: 3–3.4 MHz, II: 3.4–4 MHz, III: 4–5 MHz) to make the adjusting inductance L_0 better compensate their high capacitive reactance so that the reactance of the central frequency of each sub-band is closer to 0 Ω, the middle frequency band (IV: 5–15 MHz) and higher frequency band (V: 15–30 MHz) are divided to effectively prevent the radiation pattern from up-warping in the higher frequency band, a RF switch can be set at 5 m (1/4 wavelength at 15 MHz) to reduce its radiation height by disconnecting the upper and lower antennas.

When working in band I–IV, the radiator control switch is closed, the network control switch is switched to the corresponding band port (I–IV), and their corresponding L_0 and matching network are accessed. At this time, the reconfigurable antenna works in the corresponding band (I–IV) state; when working in band V, the radiator control switch is disconnected, and the network control switch is switched to port V, and L_0 and matching network of band V is accessed, at this time, the reconfigurable antenna works in band V state. In this way, the proposed reconfigurable antenna realizes the integration of five antennas on one antenna through RF switch control.

Antenna optimization

Whether the RL single loading, or the adjusting inductor and matching network of each sub-band, all need strong optimization algorithm to be optimized and designed. In this paper, the grasshopper optimization algorithm (GOA) [23, 24] is used to optimize the parameters of the loading network and matching network to achieve the desired design purpose.

Grasshopper optimization algorithm

GOA is a kind of natural heuristic algorithm, whose design inspiration comes from the social behavior of grasshopper in nature.

https://doi.org/10.1017/S1759078720001117 Published online by Cambridge University Press

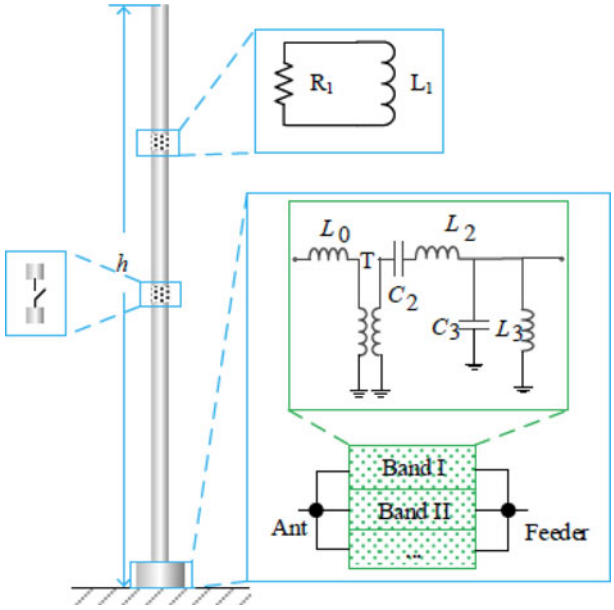

Fig. 2. Proposed frequency reconfigurable whip antenna structure.

The grasshopper swarm moves slowly and slowly in its infancy but has a wide range of activities in its adulthood. These two characteristics make two trends in the search process of the natural heuristic algorithm: exploration and exploitation, which, as well as target search, are naturally accomplished by grasshoppers. In order to solve the optimization problem for avoiding grasshoppers reaching comfort zone quickly and the population not converge to a specific point, the mathematical model for simulating grasshopper swarm behavior is revised as follows [22, 23]:

$$X_i^d = c\left(\sum_{\substack{j=1\\ j\neq i}}^{N} c\frac{ub_d - lb_d}{2}s(|x_j^d - x_i^d|)\frac{x_j - x_i}{d_{ij}}\right) + T_d, \quad (1)$$

$$s(r) = fe^{\frac{-r}{l}} - e^{-r}, \quad (2)$$

$$c = c_{max} - \frac{l(c_{max} - c_{min})}{L}, \quad (3)$$

where $X_i^d$is defined as the location of i-th grasshoppers in the d-th dimension solution space, ub_d, $lb_d$are the upper and lower bound of the d dimension solution space; d_{ij} is the distance between i-th grasshopper and j-th grasshopper, $i, j = 1, 2, \ldots, N$ (N is the population size); $s(r)$ is the force function of social activities, f, l are the attraction intensity and the attraction length between grasshoppers; T_d is the target value of the d-th dimension (best solution found so far). c is used to reduce the decline coefficients of the comfort zone, exclusion zone, and attraction zone, c_{max}, c_{min} are the maximum and minimum values of c, l is the current iteration times and L is the maximum iteration times respectively.

Equation (1) cleverly simulates the interaction between grasshoppers in a swarm. The next position of grasshoppers is determined by their current position, target position, and the position of all other grasshoppers, which is different from PSO whose next position is based on the current position, personal best, and global best, GOA requires all search agents to participate in defining the next location of each search agent. The first component of the equation takes into account the position of grasshoppers relative to other grasshoppers, the second component simulates the trend of grasshoppers transferring to food sources, the parameter c simulates the deceleration of grasshoppers approaching food sources and slowing down to eat.

The mathematical model of the GOA requires grasshoppers to move towards the target gradually during the iteration process, avoiding convergence to the target too quickly, so as to fall into local optimum. GOA saves the most promising target in the search space in each iteration and requires grasshoppers to move towards it gradually. This is to find a better and more accurate target as the best approximation of the real global optimum in the search space. Like other evolutionary algorithms, GOA uses fitness function to guide grasshoppers to search their optimal location in d-dimensional space in order to meet the requirements of the objective function. At each stage of the algorithm, the position vector corresponding to the optimal fitness value is taken as the global optimal position vector, and this information is transmitted to other grasshoppers around so that grasshoppers can adjust their steps and position vectors accordingly until they reach the target position of food. The main optimization process of GOA is shown in Fig. 3. The advantages of applying GOA to broadband antenna loading and matching network optimization have been verified in paper [25, 26], and this paper will not be repeated.

Algorithm design

For wire antenna, the solution object of moment method is generally electric field integral equation, When the length of the loading area is much smaller than that of the antenna, Dirac function can be used to replace the distribution of loading impedance in the loading area and its neighborhood. Taking the feed point at the root of the antenna as the coordinate origin and the antenna axis as the z-axis to establish the column coordinate system, the load impedance distribution of the antenna can be expressed as follows:

$$Z(z) = Z_i\delta(z - z_i), \quad (4)$$

where Z_i is the impedance of the lumped element at the loading position, z_i is the position of the loading element.

In the simulation calculation, considering that the current on the surface of the long straight wire antenna is axisymmetric with respect to the z-axis, the surface current can be equivalent to the line current on the antenna axis, that is, $I(z')\mathrm{d}z$ is used instead of $J_s(r')\mathrm{d}A'$. The antenna body will be divided into several sections, and the current on each section can be expressed by a polynomial. The current function is described as follows:

$$I_i(z') = \sum_{k=1}^{N_i} I_{i,k}\left|\frac{z'}{z_{i+1}}\right|^{k-1}, \quad (5)$$

where $z_i \le z' \le z_{i+1}$, $i = 1, 2, \ldots, N+1$ is segment number, $k = 1, 2, \ldots, N_i$;N_i is the term number of the current polynomial of the i-th segment (i.e. the segment between z_i point and z_{i+1} point); N_{i-1} is the order of the current approximate polynomial of the i-th segment.

https://doi.org/10.1017/S1759078720001117 Published online by Cambridge University Press

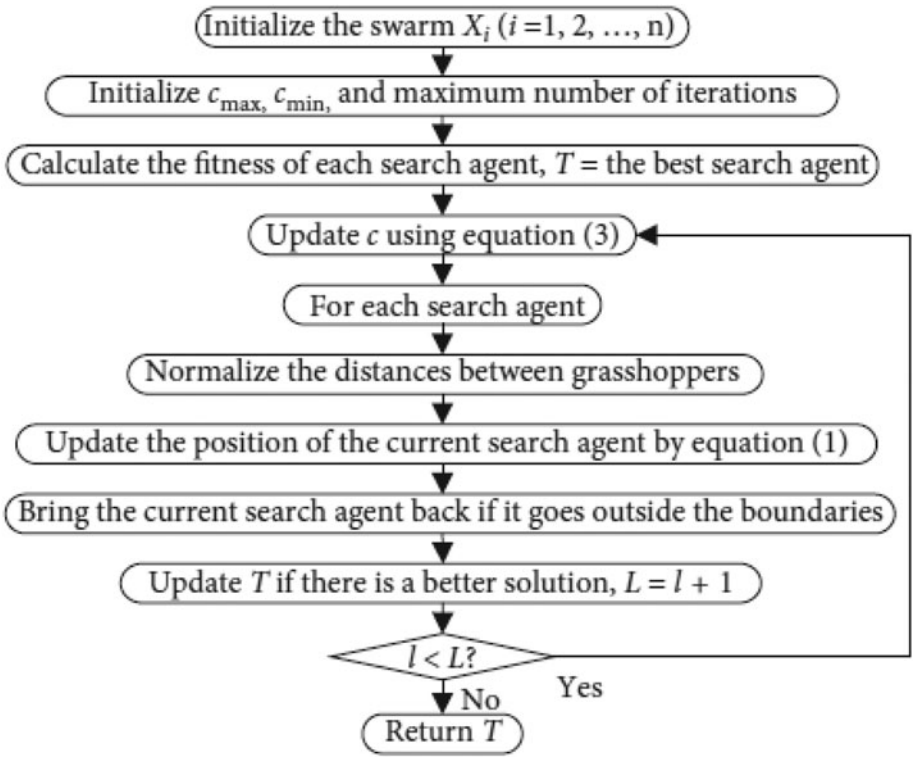

Fig. 3. Flow chart of the GOA.

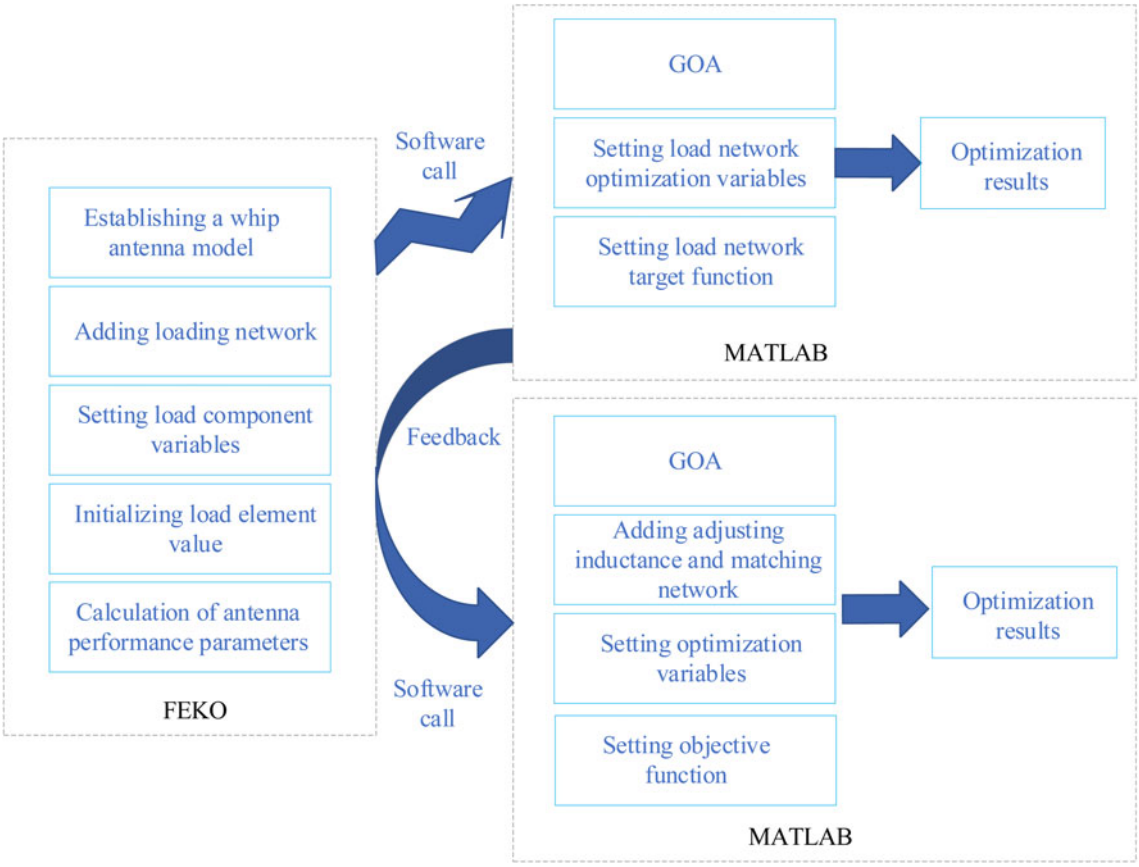

Fig. 4. Antenna calculation and optimization process.

https://doi.org/10.1017/S1759078720001117 Published online by Cambridge University Press

Table 1. Optimal values of loading

Elements	$R_1(\Omega)$	L_1 (μH)
Value	240	56

Table 2. Optimal values of L_0 and matching network for each sub-band

Band	L_0 (μH)	L_2 (nH)	C_2 (nF)	L_3 (μH)	C_3 (pF)
I	16	11	372	2.4	1000
II	12	9.1	360	1.8	1000
III	5.6	180	792	1.4	858
IV	–	0.5	160	1.1	184
V	–	150	203	0.44	54

The current expansion function is substituted into the integral equation, and the area along the antenna surface is replaced by the line integral along the antenna axis. The weight function is δ function, and a matrix equation can be obtained. Solving the matrix equation, the current distribution on the antenna can be obtained, and then the input impedance, *VSWR*, gain and pattern of the antenna can be calculated.

When studying antenna loading and broadband matching network optimization, *VSWR* and gain are generally used as performance indicators to measure the degree of optimization.

$$\Gamma(\omega_i) = \frac{Z_q(\omega_i) - Z_0}{Z_q(\omega_i) + Z_0}, \tag{6}$$

$$VSWR(\omega_i) = \frac{1 + |\Gamma(\omega_i)|}{1 - |\Gamma(\omega_i)|}, \tag{7}$$

where $Z_q(\omega_i)$ is input impedance, $\Gamma(\omega_i)$ is the reflection coefficient at ω_i, Z_0 is the feeder characteristic impedance, which is generally taken as 50 Ω.

GOA is used to improve the gain of the antenna on the premise that *VSWR* is <3 as much as possible by optimizing the loading and broadband matching network of the antenna. For the loading network, the objective function of the optimization is to minimize the maximum *VSWR* and maximize the minimum gain of each sampling frequency point [27, 28].

$$F = min\left\{\sum_{i}^{n} [W_i(VSWR(\omega_i) - 1)^2 + A_i(G_0 - G(\omega_i))]\right\}, \tag{8}$$

where $G(\omega_i)$ is the gain of antenna at i-th frequency point $\omega_i (i = 1, 2, \ldots, n)$, G_0 is rated gain, which is an adjusting parameter to weigh the broadband impedance characteristics and gain characteristics of antenna. W_i is a weighted value of *VSWR* at i-th frequency point, whose value depends on the relative importance of $VSWR(i)$. On the one hand, it retains a good *VSWR*, on the other hand, it discards a bad *VSWR*. Obviously, the smaller the value of the objective function, the better the optimization effect will be.

In order to reduce the power loss as much as possible, the matching network designed in this paper is low or even lossless,

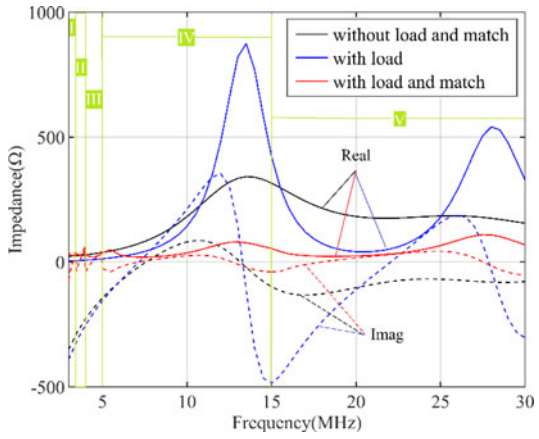

Fig. 5. Impedance curves of the proposed antenna in each sub-band.

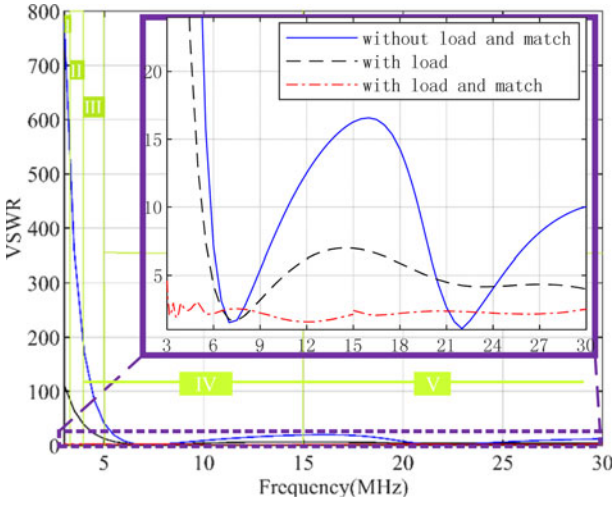

Fig. 6. *VSWR* curves of the proposed antenna in each sub-band.

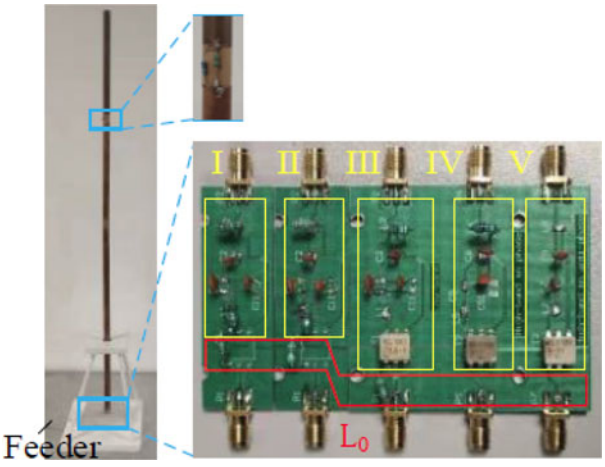

Fig. 7. Scale test antenna of the proposed antenna.

so the gain of the antenna is basically determined after loading. The matching network is only used to further reduce the *VSWR* for matching the antenna with the 50 Ω transmission line. For matching network optimization, the objective function

https://doi.org/10.1017/S1759078720001117 Published online by Cambridge University Press

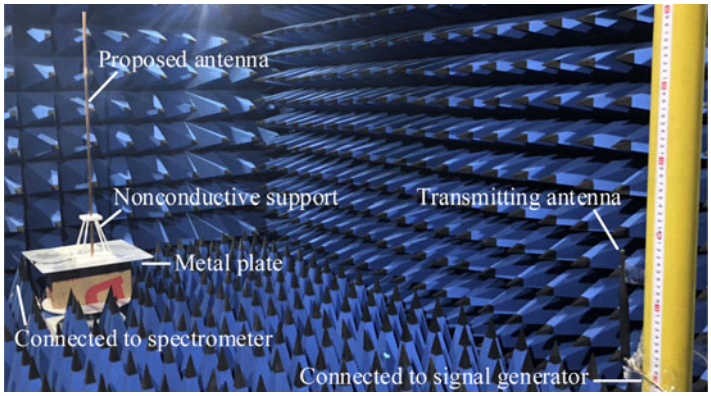

Fig. 8. Actual measurement environment of the proposed antenna.

is to minimize the average value of *VSWR*.

$$F = min\left[\sum_{i=1}^{n} VSWR(\omega_i)\right]. \quad (9)$$

Sub-band optimization

Both the loading network optimization of the upper part of the antenna and the adjusting inductance and matching network optimization of the bottom part are based on the FEKO model of the antenna. The editable program of FEKO is called by MATLAB software, and the loading and matching elements are both optimized by GOA, seeing Fig. 4 for details.

An antenna model is established with a RL loading network at 7.5 m, and the loading network parameters are optimized by equation (8). Since both the adjusting inductance and matching network are composed of lossless elements without resistance, once the loading network is determined, the gain and efficiency are basically determined. Therefore, the antenna gain should be given priority here, and the *VSWR* can be left to the matching network for further optimization. The optimized values of the loading element are shown in Table 1.

For band I–IV, connecting the upper and lower antennas at 5 m, for band V, disconnecting them, and the antenna could obtain better impedance characteristics in each sub-band by optimizing the adjusting inductance L_0 and matching network using GOA; the optimized values of the matching network elements of each sub-band are shown in Table 2. After adding the optimized loading and matching network of each sub-band, the input impedance and *VSWR* are shown in Figs 5 and 6.

It can be seen from Fig. 5 that when the loading network is added to the antenna, the input resistance of the low-frequency band increases highly (from 4 to 22.4 Ω), the capacitive reactance decreases to some extent, the change degree of input impedance in the medium and high frequency is obviously flattened, the input resistance is closer to 200 Ω, and the reactance fluctuates within the range of ±130 Ω; Moreover, the change of the input impedance of the antenna is further flattened by network matching for each sub-band, the input resistance is close to 50 Ω, and the input reactance basically fluctuates around ±40 Ω, which can better realize the impedance matching between the antenna and the feeder. As shown in Fig. 6, The *VSWR* is greatly reduced whether it is loaded or network matched, and the *VSWR* of the proposed antenna through adding load and matching network is basically <3.

Test and analysis of scaled antenna

In order to better verify the effectiveness of the proposed reconfigurable antenna, and considering the possibility of implementation, a 10:1 simple scale model is manufactured, and the electrical parameters of the scale antenna are measured.

As shown in Fig. 7, a scale-up model of 1-m reconfigurable whip antenna is established with 5 sub-bands (I–V). The frequency range is 30–300 MHz, a loading point is set at the upper part of the antenna with a parallel form of RL elements. A RF switch is added in the cavity at the middle of the antenna to control the connection of upper and lower whips in band I–IV and the disconnection of upper and lower whips in band V, and the DC control circuit of the switch enters from the bottom of the antenna and reaches the radiator control switch in the middle of the antenna through the inner cavity of the antenna. Corresponding inductance L_0 and matching network designed for five sub-bands are integrated on a 1.6 mm thick printed circuit board to simplify the circuit structure, which is placed in the antenna base. In Fig. 7, L_0 is the adjusting inductance, and the labels "I–V" respectively, represent the matching network of sub-band I–V, the transformer is connected parallel to a "r"-shaped LC network, and the power is supplied by a 50 Ω feeder. Here, a finite metal plate (iron is used in this paper) of 1 m × 1 m is selected as the ground medium.

The actual antenna is placed in the microwave laboratory to measure the performance parameters, seeing Fig. 8. In this paper, the comparison method is used to measure the antenna gain. Because the space of the microwave laboratory is relatively small, it cannot fully meet the distance requirements of the whole VHF antenna far-field test, especially the far-field measurement in the lower frequency band. In order to verify the effectiveness of the proposed antenna, only the far-field of the antenna at the higher frequency point are measured.

Figure 9 shows the characteristic curves of the proposed frequency reconfigurable antenna, including *VSWR*, gain, and efficiency. Through the simulation and measurement of the *VSWR*, it can be seen that 98% of the frequency points are <3, with an average value of 2.34, the measured value of all the frequency points is <3, with an average value of 2.14, and the measured value is consistent with the simulated one, but there is a certain fluctuation due to the impact of the environment, the *VSWR* is greatly improved in the lower-frequency band, mainly because the nonlinearity and loss of the core of the transmission line transformer can smooth the high capacitive reactance of the input end in the lower-frequency band. The gain of the proposed antenna is all >−2.5 dB, with an average of 3.90 dB, the efficiency

https://doi.org/10.1017/S1759078720001117 Published online by Cambridge University Press

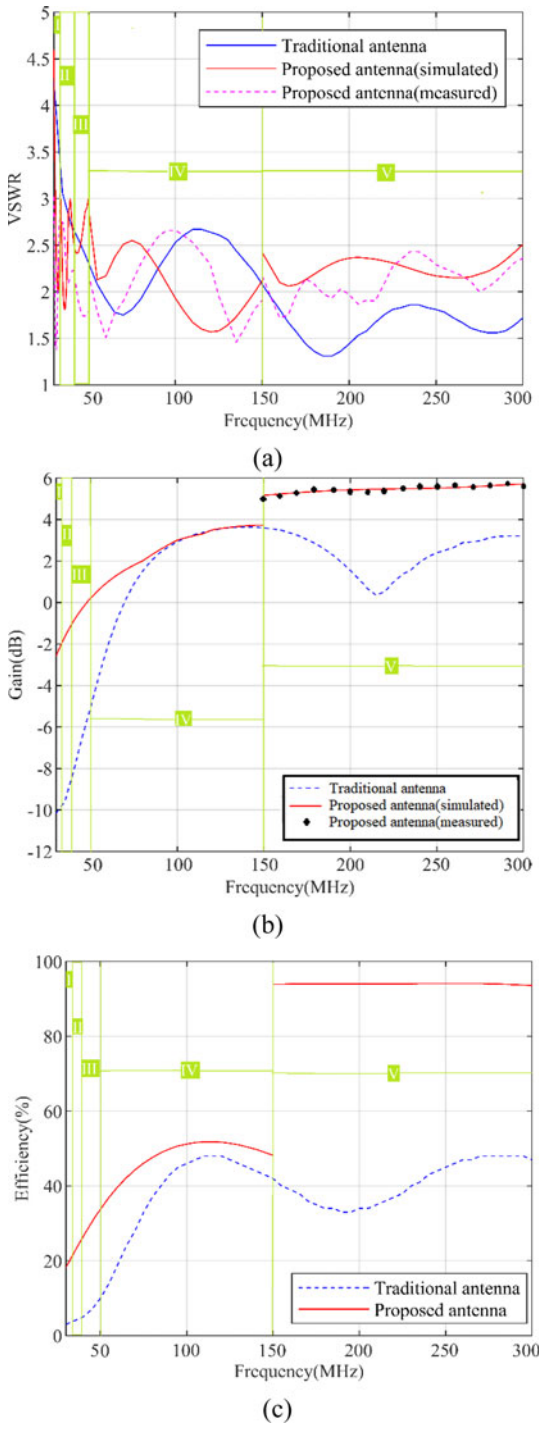

Fig. 9. Electrical performance parameters (a) *VSWR*, (b) gain, and (c) efficiency of each sub-band of the proposed antenna.

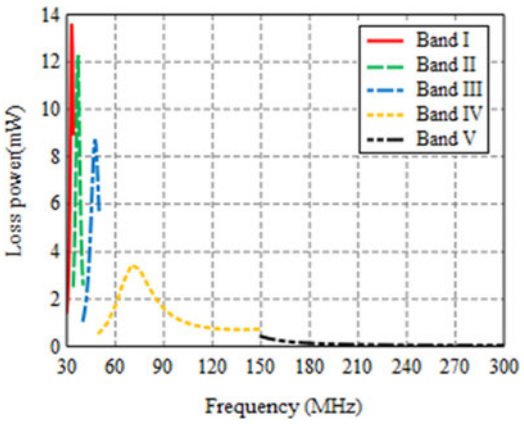

Fig. 10. Loading loss power of the proposed antenna.

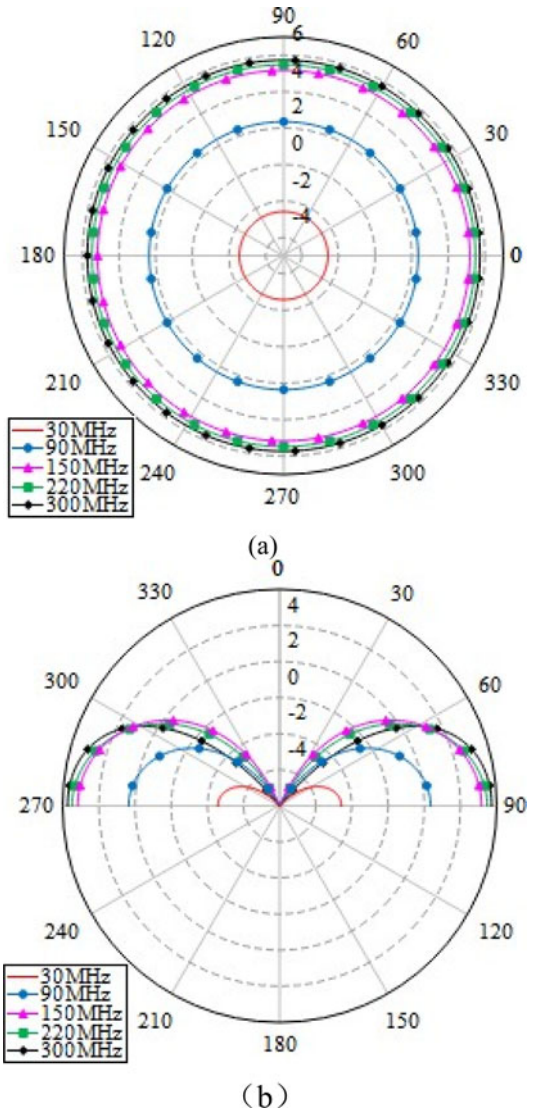

Fig. 11. (a) Horizontal pattern, and (b) vertical pattern of the proposed antenna.

is >18.2%, with an average of 71.59%, both are much higher than that of the traditional antenna. Under the existing measurement conditions, the gain of the proposed antenna in the range of 150~300 MHz is measured, and the measured value is basically consistent with the simulation value, which is slightly affected by the manufacturing accuracy.

It can be seen from Fig. 9(b) and (c) that the gain and efficiency of the frequency reconfigurable antenna increase greatly at 150 MHz, because after 150 MHz (i.e. band V), the RF switch in the middle part of the antenna is disconnected, and only the lower part of the antenna is involved in the radiation. At this time, the radiation height of the antenna is close to 1/4

https://doi.org/10.1017/S1759078720001117 Published online by Cambridge University Press

wavelength, so the antenna can get a better match. Moreover, the failure of the upper part of the antenna (contains loss resistance) to access the radiation greatly reduces the power loss of the antenna, seeing Fig. 10, so the gain and efficiency of the antenna are greatly improved in band V.

Due to the limitation of size and frequency, it is impossible to measure the far-field radiation pattern of the antenna in the microwave laboratory. Figure 11 shows the gain pattern of the proposed antenna calculated by the moment method. In the whole band, the horizontal patterns are all omnidirectional, the vertical patterns all keep the half shape of "∞", and there is no such phenomenon of up-warping as the traditional antenna, which is also consistent with the gain curve of Fig. 9(b). Therefore, the frequency reconfigurable antenna designed in this paper can achieve omnidirectional radiation with high gain and high efficiency to better realize long-range, medium-range, and short-range communication in the whole band.

Conclusion

In this paper, aiming at the problems of low gain and efficiency in low-frequency band and up warping in high-frequency band of the existing HF broadband whip antenna, the frequency reconfigurable antenna technology is introduced to divide the waveband reasonably. The antenna is composed of a low loss loading point and five lossless matching networks for five sub-bands. Through the optimization of GOA, a gain and efficiency improved frequency reconfigurable antenna is finally designed. The *VSWR* of the proposed antenna is <3, with an average value of 2.14, the gain is more than −2.5 dB, with an average value of 3.90 dB, the efficiency is more than 18.2%, with an average value of 71.59%, and the pattern keeps the horizontal omnidirectional in the whole short wave band, without the phenomenon of up-warping, whose performance of the proposed antenna is obviously better than that of the traditional antenna. The scaled prototype of the antenna is manufactured and tested, and the measured results are in good agreement with the simulation results, which proves that the proposed reconfigurable design is an effective method to realize broadband whip antenna with high efficiency.

Acknowledgement. This work was supported by Natural Science Foundation of Hubei Province under Grant 2018CFB704.

References

1. **Stutzman WL and Davis WA** (1999) *Antenna Theory, Wiley Encyclopedia of Electrical and Electronics Engineering*. New Jersey: John Wiley & Sons, Inc.
2. **Croswell W** (2003) Antenna theory, analysis, and design. *IEEE Antennas & Propagation Society Newsletter* **24**, 28–29.
3. **Lee S-W, Go H-C and Jang Y-W** (2006) A low profile wideband top - loading monopole antenna with a ring – shaped plate. *Microwave & Optical Technology Letters* **48**, 1458–1460.
4. **Lee S, Go H and Jang Y** (2006) A low profile wideband top- loading monopole antenna with a ring-shaped plate. *Microwave and Optical Technology Letters* **48**, 1458–1460.
5. **Lin B, Lin T, Ge Y and Wang RR** (2014) The top loading antenna with fractal photonic crystal used in TD-LTE system. *Advanced Materials Research* **915–916**, 1163–1166.
6. **Bevensee RM** (1989) A lower bound to the broad-band power scattered from an electrically linear antenna with a general lumped load. *IEEE Transactions on Antennas and Propagation* **37**, 555–563.
7. **Lu JH and Yang KP** (1998) Slot-coupled compact triangular microstrip antenna with lumped load. *IEEE Antennas & Propagation Society International Symposium*.
8. **Jie A, Huang J, Wu W and Yuan N** (2017) A miniaturized Vivaldi antenna by loading with parasitic patch and lumped resistor. *AEU – International Journal of Electronics and Communications* **81**, 158–162.
9. **Lau BK, Andersen JB, Kristensson G and Molisch AF** (2006) Impact of matching network on bandwidth of compact antenna arrays. *IEEE Transactions on Antennas & Propagation* **54**, 3225–3238.
10. **Rodriguez JL, Garca-Tunon I, Taboada JM and Obelleiro F** (2007) Broadband HF antenna matching network design using a real-coded genetic algorithm. *IEEE Transactions on Antennas & Propagation* **55**, 611–618.
11. **Wu ZD, Meng FY, Hua J and Chen ML** (2012) Broadband sleeve monopole with very small ground impedance matching network and resistive load. *IEEE Proceedings of 2012 5th Global Symposium on Millimeter-Waves*, pp. 88–91.
12. **Thakare YB, Wankhade PS, Vasambekar PN and Talbar S** (2013) Super wideband fractal antenna for wireless communication. *IEEE International Conference on Wireless Information Technology & Systems*, 2013.
13. **Petko JS and Werner DH** (2004) Miniature reconfigurable three-dimensional fractal tree antennas. *IEEE Transactions on Antennas & Propagation* **52**, 1945–1956.
14. **Wang CF, Kong LB, Hu FG and Yang ZH** (2012) Electrically small magneto-dielectric coated monopole antenna at HF band. *IEEE Transactions on Antennas & Propagation* **2012**, 78–79.
15. **Liu C, Liu QZ, Liang YJ and Zhang JW** (2006) Design of broadband shipboard whip-type antenna at high frequency band. *Chinese Journal of Radio Science* **21**, 955–957.
16. **Bod M, Ahmadi-Boroujeni M and Mohammadpour- Aghdam K** (2016) Broadband loaded monopole antenna with a novel on-body matching network. *AEU – International Journal of Electronics and Communications* **70**, 1551–1555.
17. **Piazza D, Kirsch NJ, Forenza A and Heath RW** (2008) Design and evaluation of a reconfigurable antenna array for MIMO systems. *IEEE Transactions on Antennas & Propagation* **56**, 869–881.
18. **Mansour A, Tayel AF, Khames A and Azab M** (2019) Towards software defined antenna for cognitive radio networks through appropriate selection of RF-switch using reconfigurable antenna array. *AEU – International Journal of Electronics and Communications* **102**, 25–34.
19. **Panagamuwa CJ, Chauraya A and Vardaxoglou JC** (2006) Frequency and beam reconfigurable antenna using photoconducting switches. *IEEE Transactions on Antennas & Propagation* **54**, 449–454.
20. **Ghanem F, Hall PS and Kelly JR** (2009) Two port frequency reconfigurable antenna for cognitive radios. *Electronics Letters* **45**, 534.
21. **Tawk Y, Albrecht AR, Hemmady S and Balakrishnan G** (2010) Optically pumped frequency reconfigurable antenna design. *IEEE Antennas & Wireless Propagation Letters* **9**, 280–283.
22. **Yu Y, Jiang X, Hui L and He S** (2011) An electrically small frequency reconfigurable antenna with a wide tuning range. *IEEE Antennas & Wireless Propagation Letters* **10**, 103–106.
23. **Saremi S, Mirjalili S and Lewis A** (2017) Grasshopper optimisation algorithm: theory and application. *Advances in Engineering Software* **105**, 30–47.
24. **Mirjalili SZ, Mirjalili S, Saremi S and Faris H** (2017) Grasshopper optimization algorithm for multi- objective optimization problems. *Applied Intelligence* **3**, 1–16.
25. **Wang H, Liu C, Wu H and Xie X** (2019) A novel frequency reconfigurable HF broadband whip antenna based on GOA optimization. *Progress In Electromagnetics Research M* **87**, 11–21.
26. **Wang H, Liu C, Wu H, Li B and Xie X** (2020) Optimal pattern synthesis of linear array and broadband design of whip antenna using grasshopper optimization algorithm. *International Journal of Antennas and Propagation* **2020**, 14–28.
27. **Wang HF, Liu C, Wu HN and Xie X** (2019) Optimization design of short wave broadband whip antenna loaded with radiation lobes. *Journal of National University of Defense Technology* **41**, 159–165.
28. **Wang H, Liu C, Wu H and Xie X** (2020) A novel broadband double whip antenna for very high frequency. *Progress In Electromagnetics Research C* **99**, 209–219.

https://doi.org/10.1017/S1759078720001117 Published online by Cambridge University Press

Hengfeng Wang received the B.Sc. degree in communication engineering from Hunan University, Changsha, China, in 2014, and the M.Sc. degree in communication and information system from the Naval University of Engineering, Wuhan, China, in 2016, where he is currently pursuing the Ph.D. degree, focusing on shortwave communications, array antenna, and broadband antenna.

Chao Liu received the B.Sc., M.Sc., and Ph.D. degrees in communication engineering from the Xi'an University of Electronic Science and Technology, in 1985, 1996, and 2009, respectively. He is currently a Professor and Ph.D. Supervisor with the College of Electrical Engineering, Naval University of Engineering. His main research interests include VLF communication, antenna design, and numerical analysis for electromagnetic fields.

https://doi.org/10.1017/S1759078720001117 Published online by Cambridge University Press